Proceedings: Fifth International Conference on Case Histories in Geotechnical Engineering
New York, NY, April 13-17, 2004

CASE STUDIES OF PILE FOUNDATIONS UNDERGOING LATERAL SPREADING IN LIQUEFIED DEPOSITS

K. Ishihara
Chuo University
Tokyo 112-8551, Japan

M. Cubrinovski
Kiso-Jiban Consultants
Tokyo 102-8220, Japan

ABSTRACT

A well-documented case study from the 1995 Kobe earthquake highlighting the performance of pile foundations in liquefied deposits undergoing lateral spreading is presented. The subject of this study is an oil-storage tank supported on 69 precast concrete piles, 23 m long and 45 cm in diameter. The tank is located in the west part of Mikagehama Island, about 20 m inland from the revetment line. During the Kobe earthquake, the fill deposit surrounding the foundation of the tank developed liquefaction. The quay wall moved seawards and consequent lateral spreading of the backfill soils affected seriously the piles supporting the tank. This paper presents results of detailed ground surveying depicting the ground distortion in the backfill soils and observations from field inspection of damage to the piles including bore-hole camera recordings and inclinometer measurements along the length of the pile. The piles were found to have suffered largest damage at depths corresponding to the interface between the liquefied fill deposit and the underlying non-liquefied soil layer. A simplified numerical analysis methodology was developed and used to perform the back-analysis for the piles damaged by the lateral spreading. The location and extent of the damage to the piles computed in the numerical analysis were shown to be in good correspondence with the actual damage observed in the field inspection of two piles of the tank foundation.

INTRODUCTION

Liquefaction of surrounding soils during earthquakes may affect the performance of pile foundations leading to damage and even collapse of piles. In fact, there are cases of liquefaction related damage to piles caused by an excessive lateral movement of the liquefied soils. Generally speaking, two different phases in the pile response have to be recognized: one is the response of piles in the course of cyclic ground movement, and the second is the pile response during the subsequent lateral spreading of the liquefied soils. This paper highlights the performance of pile foundations in liquefied deposits based on a well-documented case history from the 1995 Kobe earthquake.

The investigated oil-storage tank is supported on piles and has a 4 m wide belt of improved soil around the perimeter of its foundation. During the Kobe earthquake, the fill deposit surrounding the foundation of the tank developed liquefaction. The quay wall, located about 20 m west of the tank, moved seawards and consequent lateral spreading of the backfill soils affected seriously the piles supporting the tank. Observations from detailed field survey of the ground and inspection of the damage to the piles are first presented in this paper, followed by results of analyses for the pile undergoing lateral spreading of the liquefied soils.

MIKAGEHAMA TANK

Mikagehama is a man-made island in the port area of Kobe where a number of LPG and oil-storage tanks are installed. Its location is shown in Fig. 1. A layout of the tanks and auxiliary facilities in Mikagehama tank farm is shown in Fig. 2. The subject of this study is the oil-storage Tank TA72 which is located in the west part of the island, about 20 m inland from the revetment line. The tank has a diameter of approximately 15 m and storage capacity of 2450 kl.

Pile Foundation

Cross sectional view of the tank and its foundation is shown in Fig. 3 while plan view of the foundation is shown in Fig. 4 respectively. The tank is supported on 69 pre-stressed high-strength precast concrete piles which are 23 m long and 45 cm in diameter. At the top, the piles are embedded in a 50 cm thick concrete slab as shown in Fig. 5. In order to densify and strengthen the foundation soil, sand compaction piles had been installed around the perimeter of the tank foundation, down to a depth of approximately 15 m. Dimensions and arrangement of the compaction piles are shown in Fig. 4.

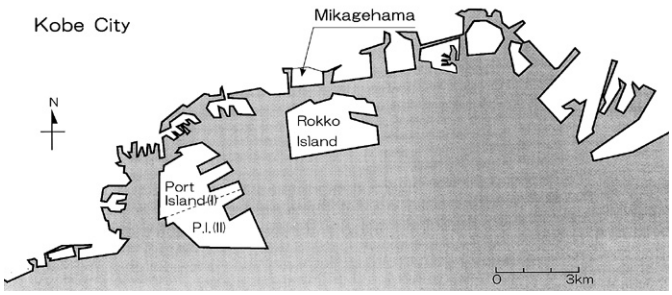

Fig. 1. Overview of reclaimed lands in the port area of Kobe

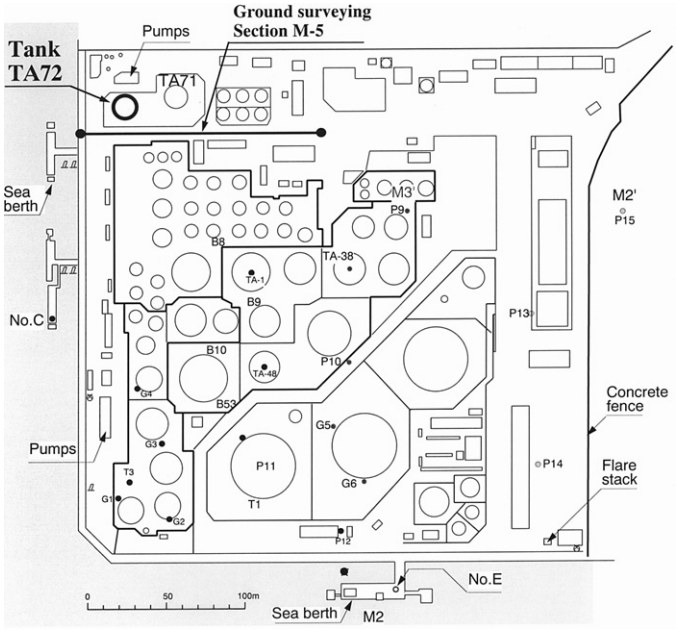

Fig. 2. Location of oil Tank TA72 at Mikagehama Island

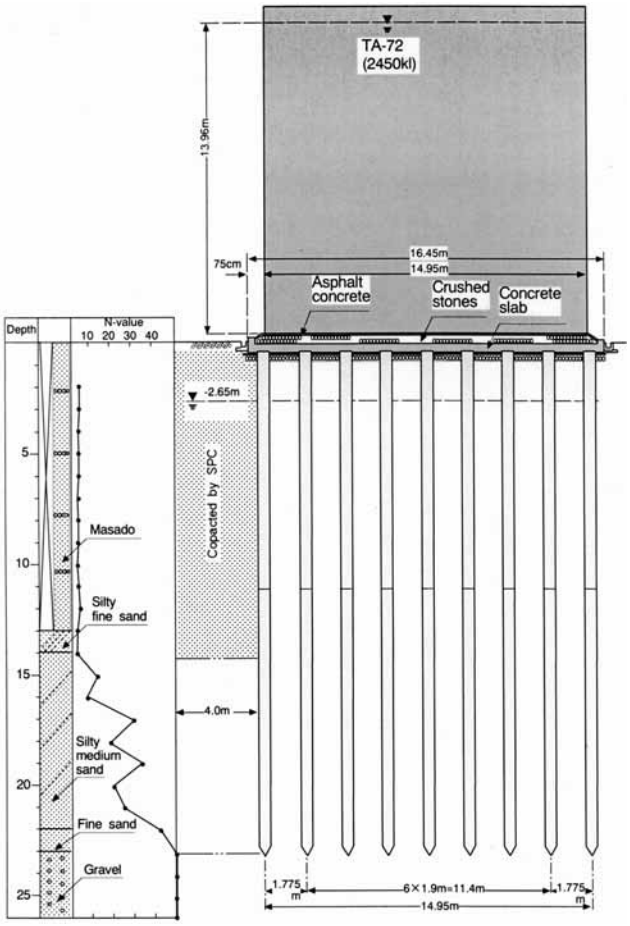

Fig. 3. Cross sectional view of Tank TA72 and its foundation

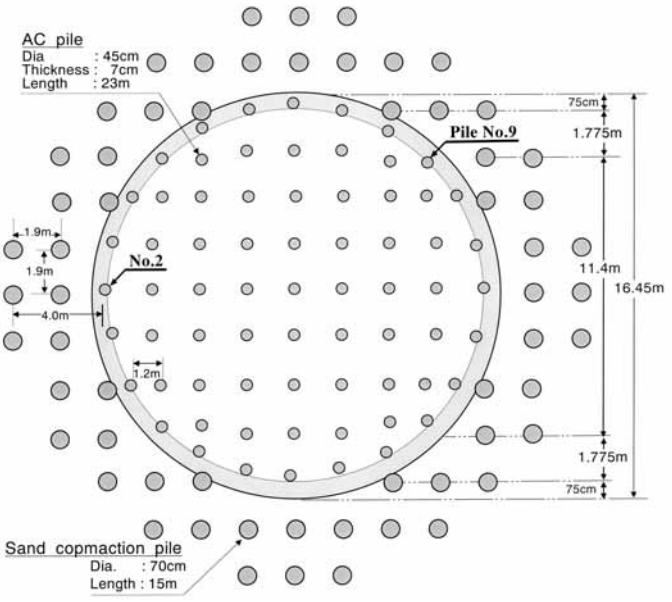

Fig. 4. Plan view of foundation

Soil Profile

Ground conditions at Mikagehama Island are typical of the landfills in the port area of Kobe, with a thick fill deposit of Masado soils (disintegrated weathered granite) overlying the original seabed layer and deep gravel layers. At the site of Tank TA72, the fill deposit and underlying silty soil layer are 13.6 m and 10 m thick respectively. The ground water level is estimated at 2.5 to 3.0 m depth. Results of SPT measurements are shown in Fig. 6 where it may be seen that the original fill deposit has a uniform and rather low SPT blow count of 5 to 6 throughout the depth (Fig. 6a). The SPT resistance in the silty layer is generally in the range between 20 and 35 blow counts except for the top 1-2 m of the layer where very low blow count has been measured. The *N* value of the deep gravel layer is 50. Standard penetration tests have also been conducted in the sand compaction pile zone (soil in-between the compaction piles) and the foundation soil (soil in-between the concrete piles). Figs. 6b and 6c show that as a result of the ground improvement, the SPT resistance of the Masado layer significantly increased and reached a value on the order of 10

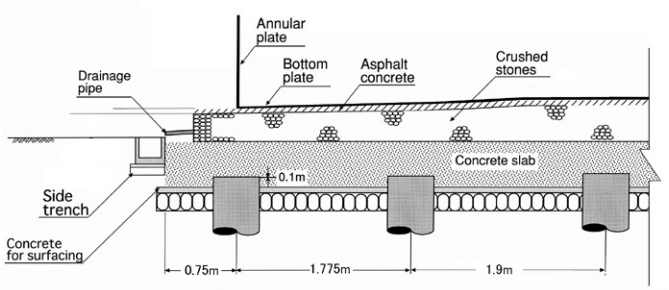

Fig. 5 Details of the foundation at the pile top

to 30 within the zone of sand compaction pile and 20 to 40 blow counts in the foundation soil respectively.

Liquefaction Strength of Fill Deposits

The fill material used for land reclamation (Masado) is a well-graded sandy soil containing a fairly large portion of gravel. The gravel fraction is commonly in the range between 30 and 50 % while the fines content is from 5 to 15 %. After the Kobe earthquake, a number of comprehensive laboratory studies were conducted to investigate undrained behavior and liquefaction characteristics of the Masado soils. Results from a series of cyclic undrained tests on undisturbed samples recovered by means of the ground freezing technique are shown in a summary form in Fig. 7. Here, the liquefaction strength showing a relationship between the cyclic stress ratio and the number of cycles required to achieve a 5 % double

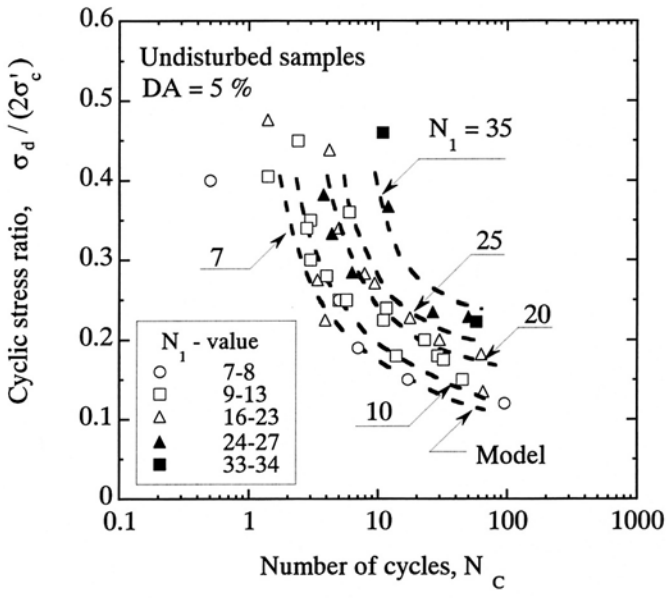

Fig. 7. Liquefaction strength of Masado soils

amplitude strain in triaxial tests is given for Masado soils with different SPT blow counts. The large variation in the SPT resistance from 7 to 34 is due to the fact that the data contain results from tests on samples secured from both undensified and densified fill deposits. It is evident in Fig. 7 that the cyclic strength of Masado soils substantially increases with the SPT blow count.

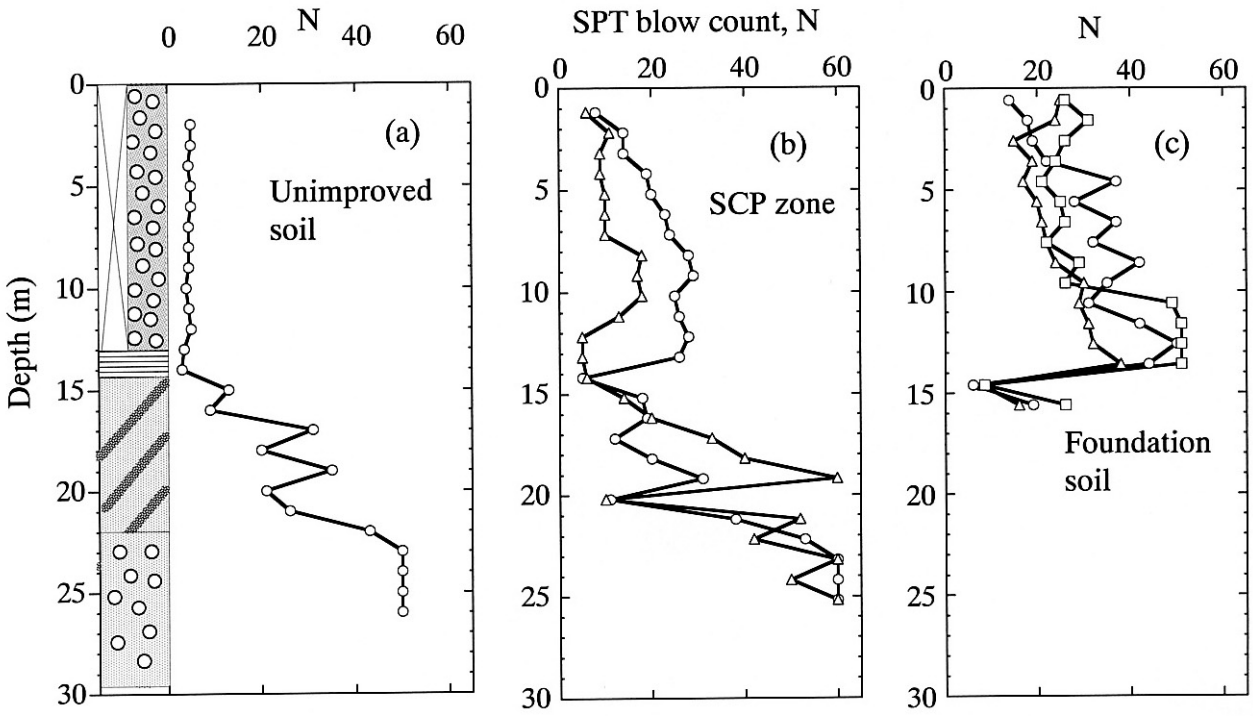

Fig. 6. SPT profiles at the site of Tank TA72: (a) unimproved soil; (b) SCP zone; (c) foundation soil

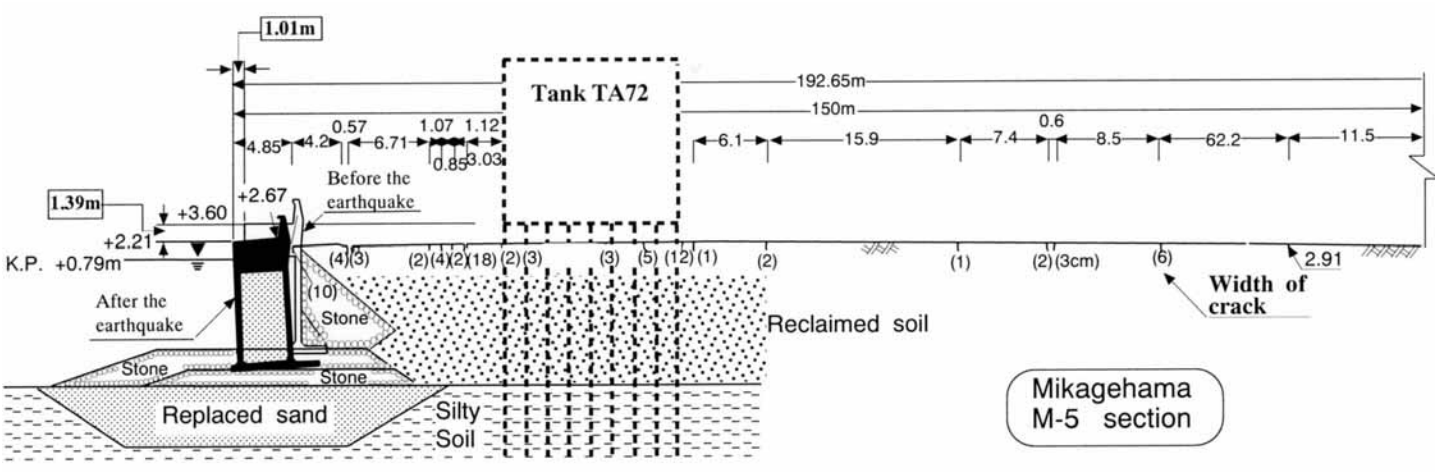

Fig. 8. Detailed profile of the quay wall movement and ground distortion in the backfills at Section M-5

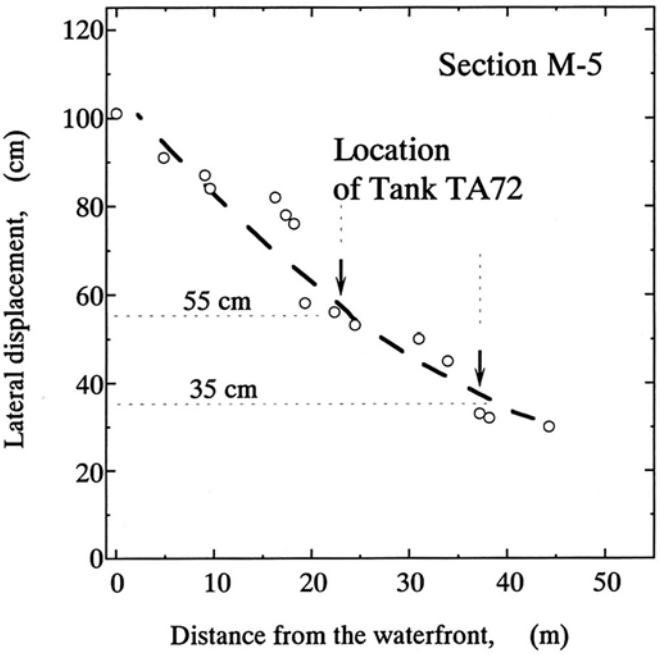

Fig. 9. Lateral ground displacement versus distance from the waterfront along Section M-5

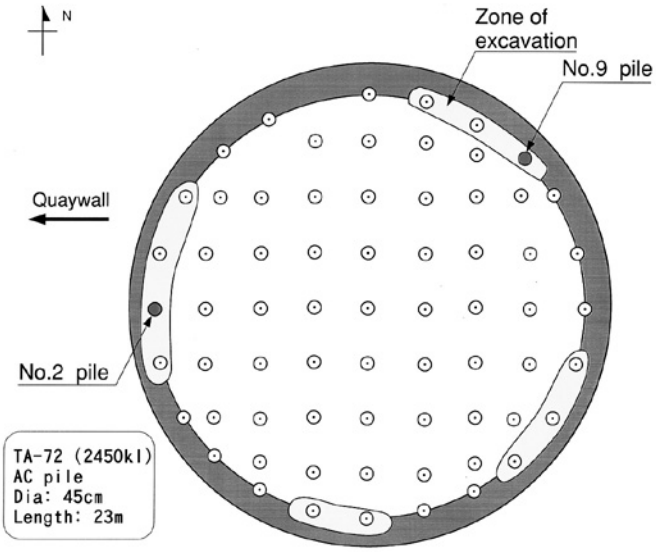

Fig. 10. Excavated trenches for visual inspection of the upper part of the piles

DAMAGE FEATURE

Ground Deformation

During the Kobe earthquake, extensive liquefaction developed in the fill deposits of Mikagehama Island resulting in scattered sand boils, lateral movements and settlement of the ground. Ishihara et al. (1997) presented results of detailed field survey on the displacement of the quay wall and distortion of the ground surface along the M-5 section which is located in the vicinity of Tank TA72, as shown in Fig. 2. The results of the ground survey are displayed in Fig. 8 where it may be seen that the quay wall moved approximately 1 m towards the sea. The seaward movement of the quay wall was accompanied by lateral spreading of the backfill soils resulting in a number of cracks on the ground inland from the waterfront. By summing up the width of the crack openings measured along the M-5 section, the lateral ground displacement was obtained and it was plotted as a function of the distance from the waterfront, as shown in Fig. 9. As indicated in this figure, the permanent lateral ground displacement corresponding to the location of Tank TA72 is seen somewhere between 35 and 55 cm.

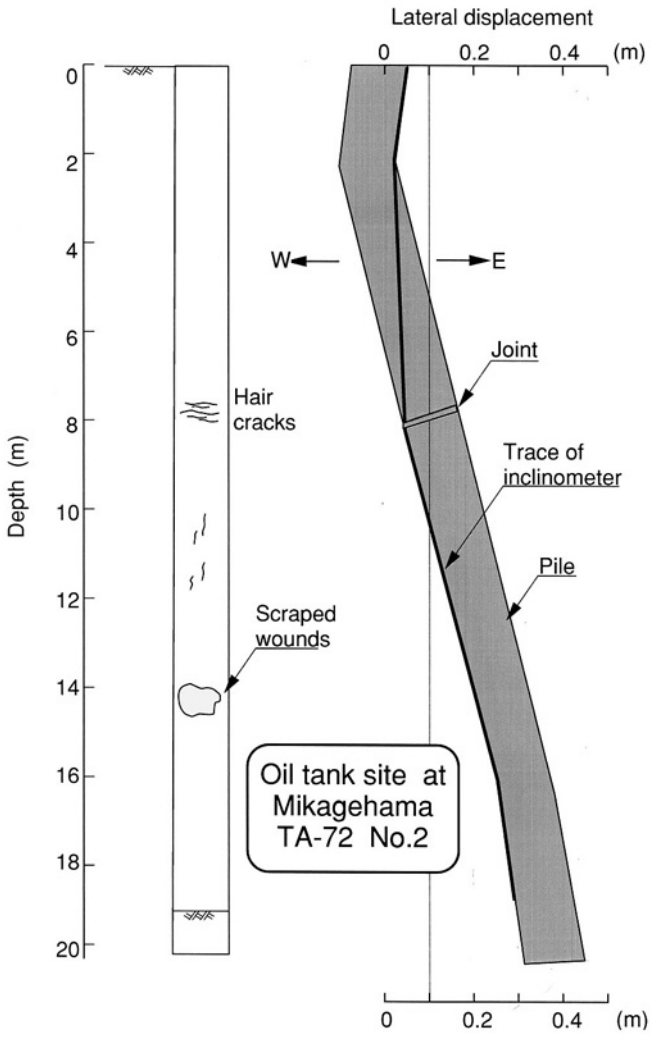

Fig. 11. Lateral displacement and observed cracks on the inside wall of Pile No. 2

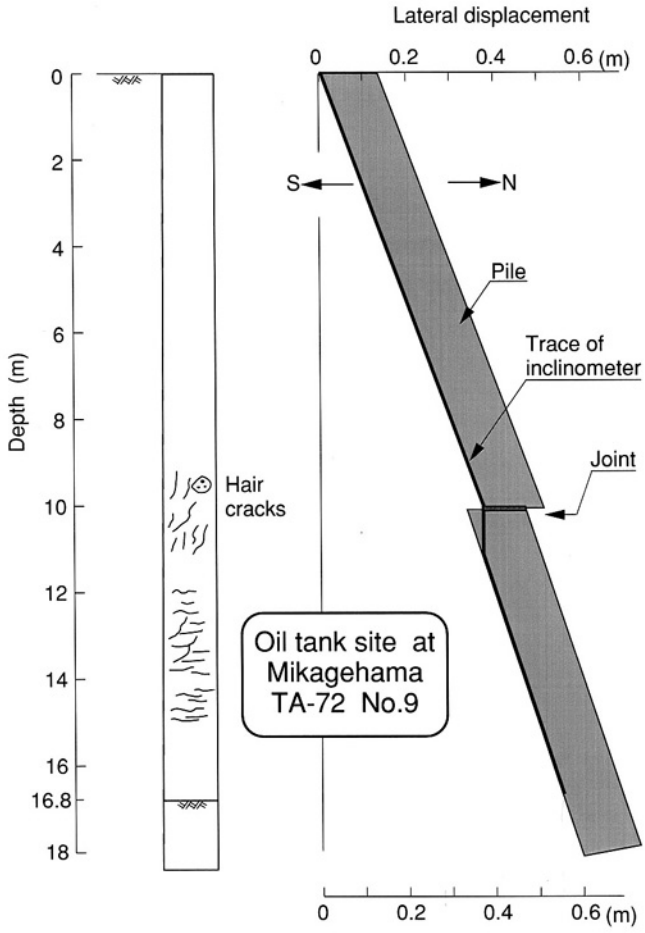

Fig. 12. Lateral displacement and observed cracks on the inside wall of Pile No. 9

Damage to Piles

To inspect the damage to the piles, a detailed field investigation was conducted on two piles of Tank TA72. The investigated piles No. 2 and No. 9 are indicated in Fig. 4. Trenches 70 cm wide and 1 m deep were excavated at 4 sections shown in Fig. 10, and the upper portion of the pile was exposed. The wall of the cylindrical piles was cut to open a window about 30 cm long and 15 cm wide. From this window, a bore-hole camera was lowered through the interior hole of the hollow cylindrical piles to examine the damage to the piles throughout the depth. The outcome of the bore-hole camera recordings is shown in Figs. 11 and 12 for the pile No. 2 and No. 9 respectively together with the inclination of piles measured by means of the inclinometer lowered into the central hole of the pile. It may be seen in these figures that the piles developed multiple cracks and suffered largest damage at a depth of approximately 8 to 14 m, which corresponds to the

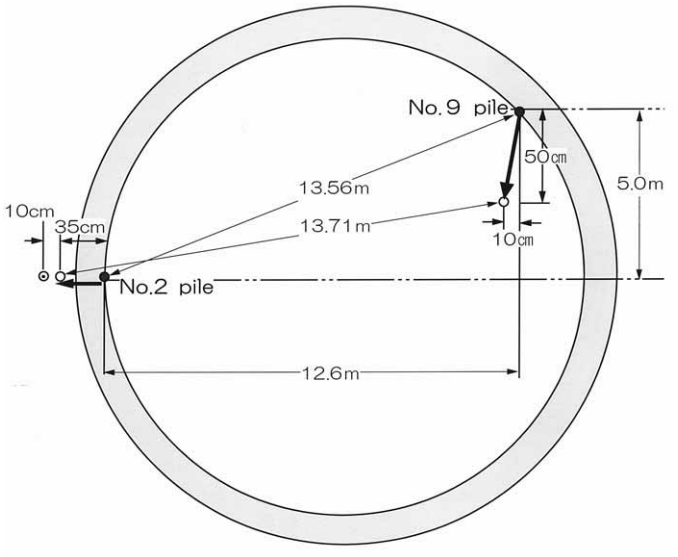

Fig. 13. Permanent lateral displacements of Pile No. 2 and Pile No. 9 at the head of the pile

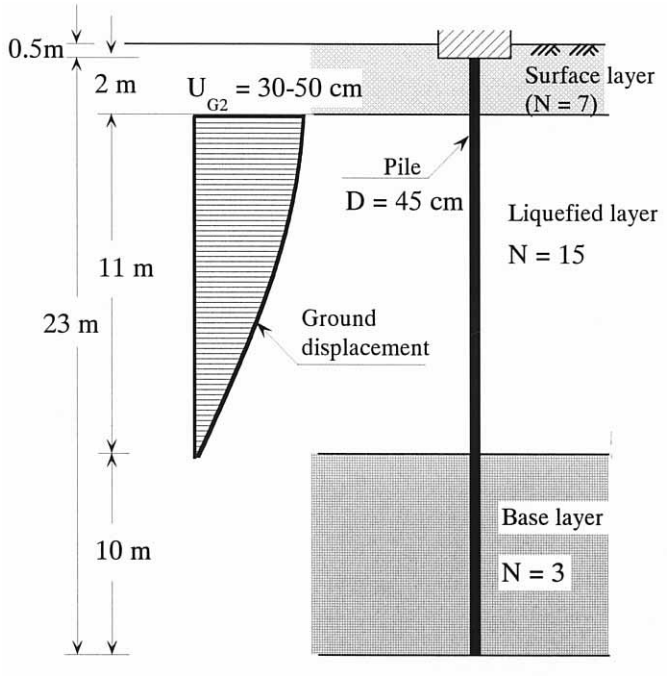

Fig. 14. Soil-pile model used for evaluating the pile response to lateral spreading

depth of the interface zone between the liquefied fill deposit and underlying silty soil layer. The observed permanent horizontal displacements at the head of the piles are shown in plan-view of Fig. 13.

SIMPLIFIED ANALYSIS OF PILES

Soil-Pile Model

A simplified approach was adopted to analyze the response of the piles due to the lateral spreading of the liquefied soils. Based on the general differential equation for piles under lateral loading, a closed-form solution was derived for a three-layer soil-pile model (Cubrinovski and Ishihara, 2002) where a liquefied layer undergoing lateral spreading is sandwiched between a non-liquefied surface layer and non-liquefied base layer. In this model, a lateral displacement on the ground surface is to be given based on some assumption arising from results of measurements. The lateral displacement of the soil in the surface layer is assumed to take a constant value throughout the depth and the displacement of the liquefied layer is assumed to have the same value at its top as the surface layer and decrease with depth with a cosine distribution.

The simplified soil-pile model for Tank TA72 is shown in Fig. 14. In the model, it is postulated that the non-liquefied layer near the ground surface and the base layer exhibit a bi-linear pressure-displacement relation as shown in Figs. 15a and 15c respectively. The liquefied soil, on the other hand, is

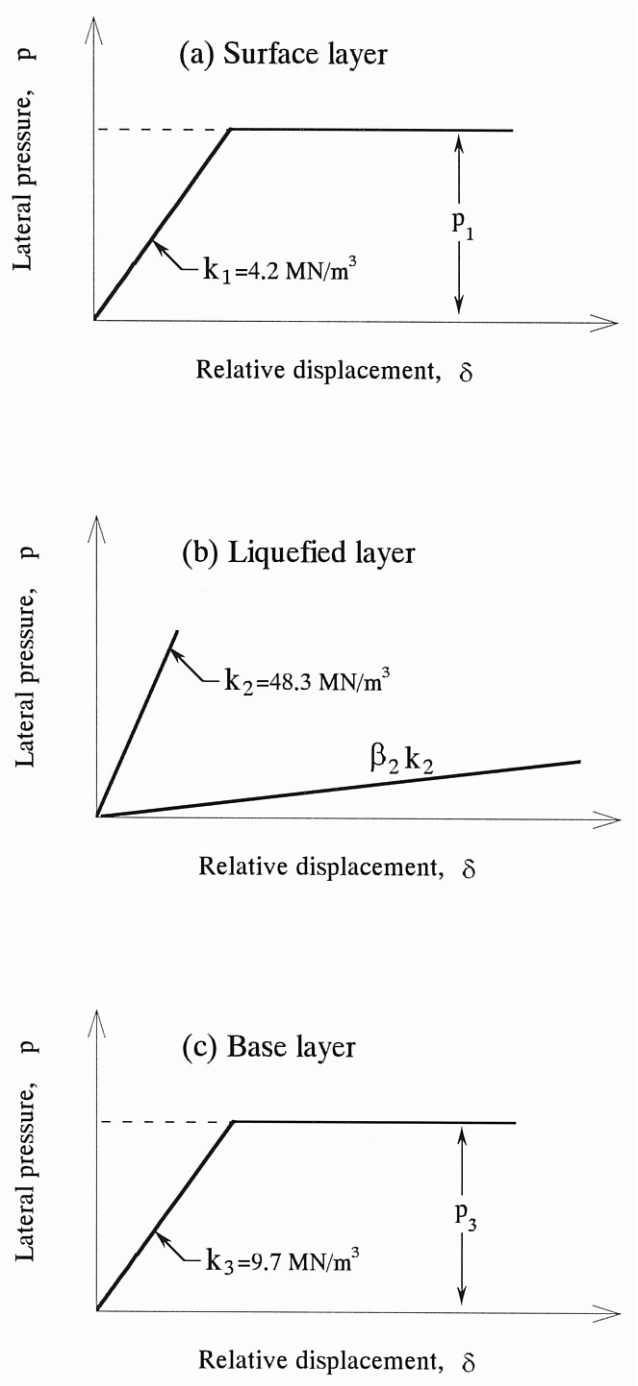

Fig. 15. p-δ relationships used for characterization of soil behavior: (a) crust layer; (b) liquefied layer; (c) base layer

represented by an equivalent linear p-δ relationship or secant stiffness ($\beta_2 k_2$), as shown in Fig. 15b, that takes into account the significant reduction in stiffness due to soil liquefaction by way of the degradation factor β_2. The subgrade reaction coefficients k_1, k_2 and k_3 were evaluated according to an empirical correlation between k and the SPT blow count N stipulated in the Japanese design code for Highway Bridge Foundations (JRA, 1980). The bending stiffness of the pile is

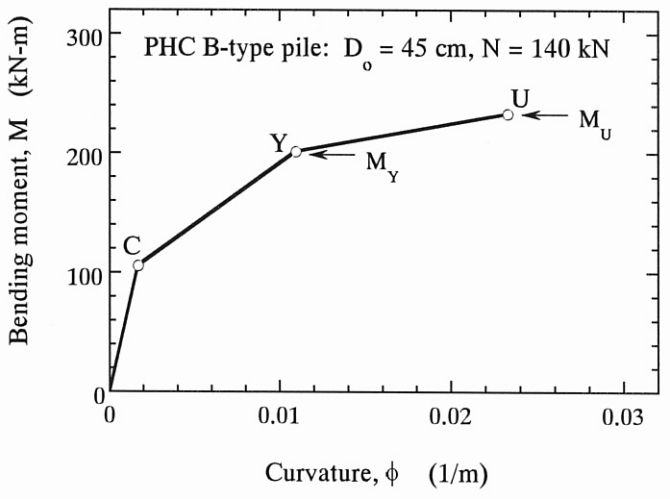

Fig. 16 Tri-linear M-ϕ relationship of the pile

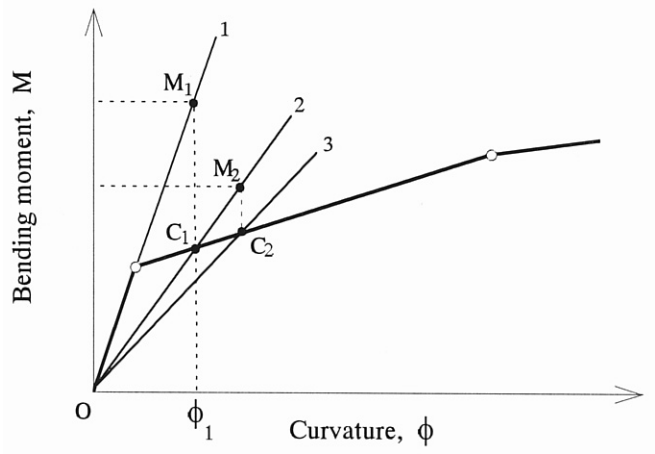

Fig. 17 Schematic illustration of the iterative calculation procedure

assumed to be represented by a tri-linear relation between the bending moment, M, and curvature, ϕ, of the pile, as shown in Fig. 16. While the bilinear p-δ relationships and tri-linear M-ϕ relationship are used to characterize the behavior of the non-liquefied soil layers and the pile respectively, the calculation is in fact performed iteratively in an equivalent linear fashion, as summarized below. The development and description of the equivalent linear procedure is given in Cubrinovski and Ishihara (2003).

Equivalent Linear Analysis Procedure

The equivalent linear analysis of the pile consists of several steps, as follows.

Step 1 … First of all, on the basis of the observed lateral ground displacements shown in Fig. 9, the magnitude of the lateral displacement at the ground surface was chosen to be 40 cm. It was also assumed that the subgrade reaction coefficient of the liquefied layer k_2 is reduced by a factor of β_2 = 1/100. For the adopted soil-pile model shown in Fig. 14 and the above assumptions, an elastic linear analysis of the pile was made using the initial stiffness for the pile and non-liquefied base layer. In this analysis, effects of the surface layer on the pile response were ignored by postulating that the lateral force in the non-liquefiable surface layer is zero. As a result of the elastic analysis, bending moments and lateral pile displacements throughout the entire length of the pile are obtained.

Step 2 … Suppose the bending moment at a certain depth computed in the first step is M_1, as illustrated in Fig. 17. The curvature corresponding to this bending moment ϕ_1 is used to determine the point C_1 on the moment-curvature relationship, as indicated by the intersection of the vertical line with the tri-linear M-ϕ relationship in Fig. 17. In the subsequent linear analysis (second iteration), the bending stiffness represented by the line OC_1 is utilized for the pile, together with a new secant stiffness for the base layer identified in the same fashion. This iterative calculation is repeated several times until convergence has been achieved. Note that throughout this phase of computation, the lateral force acting on the pile in the surface layer is kept equal to zero.

Step 3 … It is assumed that the surface layer is moving seawards along with the movement of the underlying liquefied deposit. Therefore, the lateral displacement of the surface layer is taken as being equal to the horizontal displacement at the top of the liquefied deposit. As a result of the pile analysis in Step 2, the lateral deformation of the pile in the surface layer has been obtained, and consequently, the relative displacement between the pile and the surrounding soil in the surface layer would be known. With reference to the load-deformation characteristics of the surface soil as shown in Fig. 15a, it is possible to calculate the lateral pressure on the pile throughout the depth in the surface layer that corresponds to the above relative displacements. It is to be remembered here that the lateral pressure had been assumed equal to zero throughout the calculations in Step 1 and Step 2, and therefore, an additional iterative computation becomes necessary to adjust the discrepancy between the applied load in the analysis and that resulting from the analysis. To achieve this, a second round of iterative computation is conducted. In this round of analyses, some percentage of the lateral force obtained above is applied to the pile in the surface layer, and the same procedure as in Step 2 is followed, the difference being the presence of some lateral force on the pile in the surface layer. It is to be noted that in this second round of analyses, the equivalent bending stiffness of the pile and secant stiffness of the base layer established in Step 2 are used as starting properties in the iterative procedure.

Step 4 … As a result of the second-round analysis, the deflection of the pile is re-evaluated and a modified value of the relative displacement between the pile and soil in the surface layer is determined. Using this renewed relative

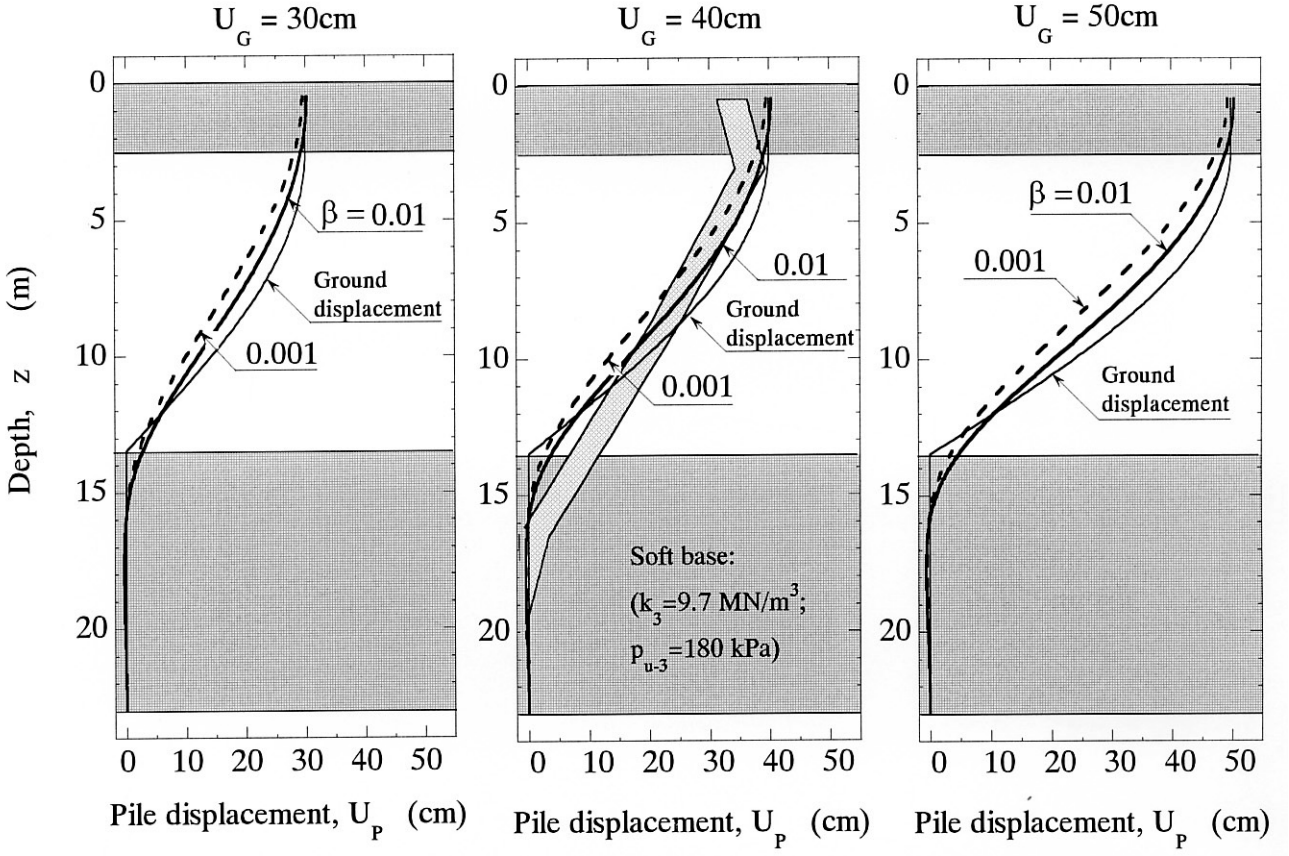

Fig. 18. Computed pile displacements in analyses with applied ground displacements of 30, 40 and 50 cm

displacement and the bilinear p-δ relationship of the crust layer shown in Fig. 15a, the corresponding lateral load on the pile is calculated. Note that this lateral load would be still different from the one assumed for this second round of the analysis.

Step 5 … The lateral load in the surface layer is again incrementally modified and the third round of analysis is performed. Such global round of analysis is repeated in an iterative manner until eventually convergence is achieved for the lateral load on the pile in the surface layer. As a final result of the equivalent linear calculation as above, a pile response is evaluated eventually where the effects of nonlinear behavior could be incorporated for all three layers of the soil deposit as well as for the pile itself.

Following the above procedure, the pile response was evaluated in this study for an assumed lateral displacement at the ground surface of U_G = 30, 40 and 50 cm, respectively, and the stiffness degradation in the liquefied soil of β_2 = 1/100 and 1/1000.

Computed Pile Response

The results of computed pile displacements are shown in Figs. 18a through 18c for the three cases where the ground displacement was assumed as 30, 40 and 50 cm respectively. For purpose of comparison, the measured displacements of Pile No. 2 are quoted from Fig. 11 and superimposed in Fig. 18b. A reasonably good agreement between the computed and observed displacements of the pile is seen in this figure. The displacement of Pile 9 was directed almost perpendicular to the direction of the lateral flow as seen in Fig. 13. This appears to have resulted from complex interaction between the pile and the foundation slab atop.

Looking over the results of the back-calculation in Fig. 18, one can recognize that the computed displacement at the pile head is nearly equal to the applied displacement at the ground surface. The same scheme of analysis was implemented also for the case of β_2 = 1/1000. The result of this analysis is shown in Fig. 18 together with the case of β_2 = 1/100. It may be seen from the results of the analyses with β_2 = 1/100 and β_2 = 1/1000 that the pile response is not very sensitive on the value of β_2. It is important to recognize however that while the eventual pile displacements are similar for the cases of β_2 = 1/100 and 1/1000, the causative loads for the pile response are different between these two cases. Namely, in the case of β_2 = 1/100, even though the stiffness of the liquefied soil is reduced significantly, the major driving force on the pile comes from the soil in the liquefied layer. Therefore, the lateral load from

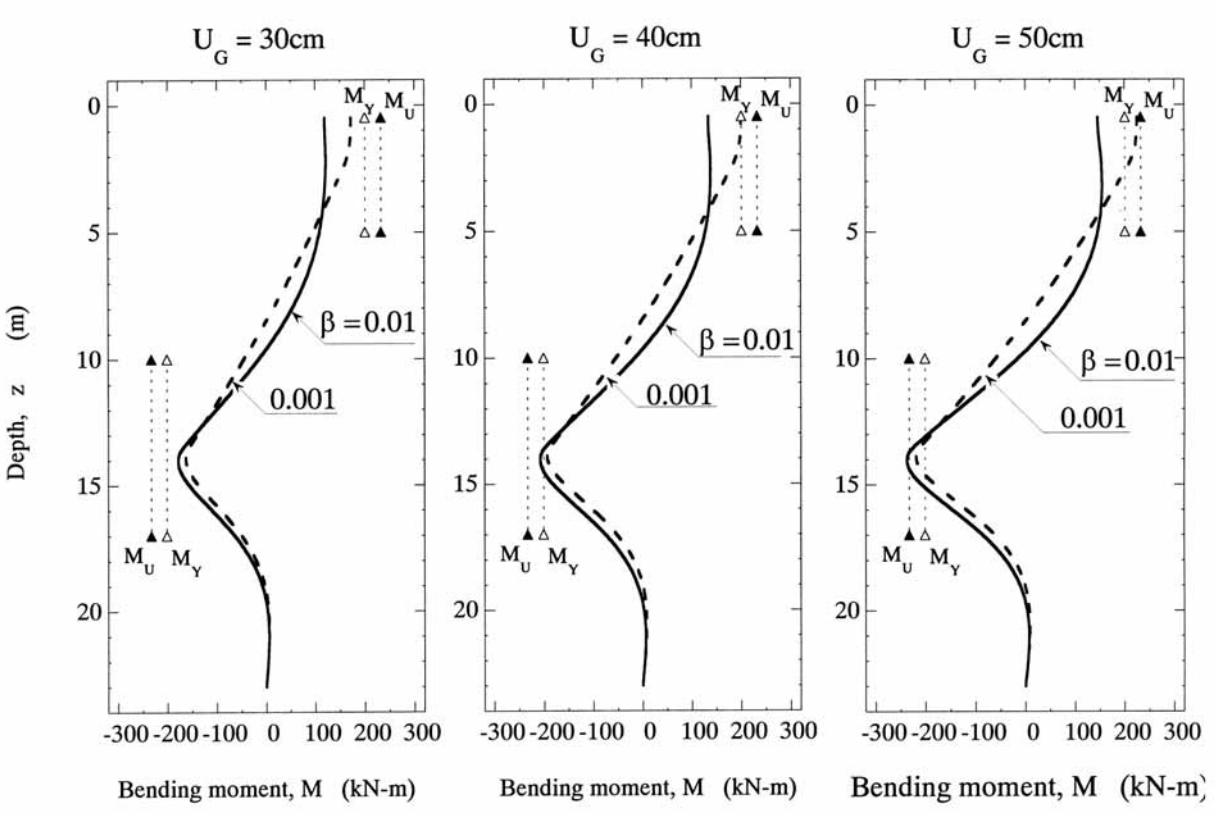

Fig. 19. Computed bending moments in analyses with applied ground displacements of 30, 40 and 50 cm

the surface layer on the pile is very small and close to zero. Conversely, in the case of β_2 = 1/1000, the liquefied layer has so small rigidity that the response of the pile is dominated by the force coming from the surface layer.

In accordance with the pile displacements as above, the computed bending moments are seen to increase with the increasing magnitude of the ground displacement as shown in Figs. 19a-19c. The maximum bending moment develops near the interface between the liquefied layer and underlying non-liquefied base layer, at depths of about 12 m to 15 m. The magnitude of the computed bending moments and their distribution throughout the depth are found to be in good correspondence with the damage to the piles observed in the field inspection as presented in Figs. 11 and 12.

CONCLUDING REMARKS

A well-documented case study from the 1995 Kobe earthquake highlighting the performance of pile foundations undergoing lateral spreading in liquefied deposits has been presented. Results of ground surveying and field inspection of piles depicting the damage features are also presented.

The piles are known to have suffered largest damage at depths corresponding to the interface between the liquefied fill deposit and the underlying non-liquefied soil layer. The location and extent of the damage to piles computed in the numerical analyses are in good correspondence with the actual damage features observed in the field inspection of two of the piles of Tank TA72.

ACKNOWLEDGMENTS

The data on soil profiling and damage features were provided by MC-Terminal Co. The authors wish to acknowledge its cooperation.

REFERENCES

Cubrinovski, M. and Ishihara, K. [2002]. “Pile response to lateral spreading of liquefied soils: Demand-Capacity Method” *Proc. U.S.-Japan Seminar Seismic Mitigation in Urban Area by Geotechnical Engineering*, Anchorage, Alaska, CD-ROM.

Cubrinovski, M. and Ishihara, K. [2003]. “Simplified method for analysis of piles undergoing lateral spreading in liquefied soils,” submitted to *Soils and Foundations*.

Ishihara, K., Yoshida, K. and Kato, M. [1997]. “Characteristics of lateral spreading in liquefied deposits during the 1995 Hanshin-Awaji Earthquake,” *Journal of Earthquake Engineering*, 1(1): 23-55.

Japan Road Association, 1980: Specification for road bridges, Vol. IV (in Japanese).